



Poly(ether-anhydride) dry powder aerosols for sustained drug delivery in the lungs

Jennifer Fiegel, Jie Fu, Justin Hanes*

*Department of Chemical and Biomolecular Engineering, The Johns Hopkins University,
3400 N. Charles Street, Baltimore, MD 21218, USA*

Received 29 January 2004; accepted 20 February 2004

Abstract

A new family of biodegradable ether-anhydride polymers was used to develop microparticles capable of controlled drug release and inhalation as a dry powder. The polymers are composed of various ratios of sebacic acid (SA) (to render the polymer insoluble in water) and poly(ethylene glycol) (PEG) (to reduce particle clearance by macrophages and improve aerosolization). Particle aerodynamic diameter was controlled within the respirable range by producing geometrically large, but low density particles as a first step toward reducing particle adhesion forces that limit efficient aerosolization of dry powders. Particles made from a variety of polymer compositions possessed high emitted doses (>80%) from a Spinhaler dry powder inhaler (DPI). Control over particle surface and bulk properties (surface roughness, surface charge, density and water retention) was achieved by varying the percentage of PEG in the polymer backbone. The addition of 10% PEG into the polymer backbone significantly enhanced deposition in the lower stages of an in vitro lung model following aerosolization from the DPI (fine particle fractions [FPF] reached 30%). Efficient aerosolization from an obsolete DPI combined with the ability to evade phagocytic clearance and provide controlled release of various drug molecules make these particles promising for prolonged drug delivery in the lung. © 2004 Elsevier B.V. All rights reserved.

Keywords: Aerosolization; Microparticle; Lung; Drug delivery; Polymers; Surface properties; PEG

1. Introduction

Pulmonary drug delivery to non-invasively and systemically administer small drugs and proteins has reached Phase III clinical trials for drugs such as insulin, calcitonin, interferons, parathyroid hormone and leuprolide [1–5], and many drugs are in earlier clinical or preclinical stages of development. Howev-

er, much less attention has been given to the possibility of using the lungs as a portal for controlled drug release and absorption that is extended over many hours to days, where the drug is protected from degradation or premature clearance by a suitable delivery system. Polymer particles are often needed to achieve these types of advanced, controlled-release drug delivery [6,7].

A new family of high molecular weight polymers designed for controlled drug delivery following inhalation or injection, the poly(ether-anhydrides), has been developed recently [8]. These materials show promise for use in the lungs for

* Corresponding author. Tel.: +1-410-516-3484; fax: +1-410-516-5510.

E-mail address: hanes@jhu.edu (J. Hanes).

several reasons: (i) they are composed of chemical species that are known to be safe in humans for various applications, poly(ethylene glycol) (PEG), sebacic acid (SA) and 1,3-bis(carboxyphenoxy)propane (CPP); (ii) their erosion times can be controlled over periods ranging from hours to several weeks by varying their monomer composition, thereby regulating the release of entrapped therapeutics; (iii) they deliver drugs with molecular weights ranging from 443 to over 5×10^6 Da in a continuous fashion for up to 7 days [9], whereas commonly used PLGA polymers often release drugs in a triphasic manner [10]; and (iv) the addition of PEG into the polymer backbone can decrease particle clearance rates by phagocytosis in the deep lung. However, effective aerosolization of particles made using the ether-anhydride family of polymers is necessary to realize their potential benefits for controlled drug delivery via the lungs.

Aerosolization and lung deposition of microparticles are significantly affected by particle physical and chemical properties [11]. The key physical parameter that predicts the site of aerosol deposition within the lungs for particles larger than several hundred nanometers is the aerodynamic diameter (d_{aero}) [12]. Even with an optimized aerodynamic diameter, however, particle surface properties can cause significant aggregation of micron-sized particles, reducing the efficiency of deep lung deposition. Surface properties, such as hydrophilicity, rugosity and charge, control interparticle adhesion forces that influence dry powder aerosolization from an inhaler and, subsequently, deposition in the lungs [11].

In this paper, control of poly(ether-anhydride) particle surface properties is obtained by simply varying the PEG content of the polymers used to produce aerosol particles. Fine particle fractions (FPF) initially increase as the percentage of PEG increases (up to 10% PEG by weight), and then decrease as the PEG percentage is raised to 30% w/w. The effect of PEG on particle surface properties, including contact angle and surface charge, and particle bulk properties, such as density and water content, are determined to aid in the interpretation of the interparticle surface forces that may control poly(ether-anhydride) particle aerosolization.

2. Materials and methods

2.1. Materials

Sebacic anhydride (acyl-SA) and polyethylene glycol anhydride (acyl-PEG8000) were synthesized as previously described [8]. PEG had a molecular weight of 8000 Da prior to acylation. Polyvinyl alcohol (PVA; 88 mol% hydrolyzed, $M_w = 78$ kDa, Polysciences, Warrington, PA), bovine serum albumin (BSA) (Sigma, St. Louis, MO), FITC-Dextran ($M_w = 20$ kDa, Sigma), lactose (Sigma) and other reagents were used as received without further purification.

2.2. Polymer synthesis

Acyl-PEG and acyl-SA powders were mixed in defined ratios in round-bottom flasks equipped with a stopcock adapter and polymerized by melt polycondensation at 180 °C under high vacuum for 30 min. Briefly, the flask was immersed in an oil bath maintained at 180 °C and the monomers were allowed to melt. High vacuum was applied (~ 0.04 – 0.05 torr) and the condensation byproduct, acetic anhydride, was collected in a liquid nitrogen trap. The polymers were allowed to cool completely at the end of the reaction and they were then dissolved in chloroform. The solution was precipitated dropwise into excess petroleum ether. The precipitate was collected by filtration and dried under vacuum to constant weight.

2.3. Polymer molecular weight analysis

The molecular weight and polydispersity of the polymers were determined by gel permeation chromatography (GPC) using a JASCO PU-980 intelligent HPLC pump, 1560 intelligent column thermostet and RI-1530 intelligent refractive index detector (JASCO, Easton, MD). Samples were filtered and eluted in chloroform through a series of Styragel columns (guard, HR4 and HR3 Waters Styragel columns) at a flow rate of 0.3 ml/min. Weight- and number-average molecular weights were determined relative to polystyrene standards (Fluka, Milwaukee, WI).

2.4. Polymer contact angle measurements

The relative polymer hydrophobicity was determined by contact angle measurements (Remé-Hart Contact Angle Goniometer, Mountain Lakes, NJ). Uniform polymer surfaces were obtained by film casting a solution of polymer dissolved in chloroform onto glass slides, followed by evaporation of the chloroform. A 20- μ l drop of water was pipetted onto the polymer surface and the contact angle measured. Reported values represent the average of 4–10 samples.

2.5. Microparticle preparation

Poly(ether-anhydride) microparticles were made by a double-emulsion solvent-evaporation technique [7,13]. To form the primary water-in-oil emulsion, 200 μ l of a 75 mg/ml BSA solution was emulsified into 4 ml of 50 mg/ml polymer solution in methylene chloride (+3 mg/ml DPPC and 3 mg/ml rhodamine B base) on ice by probe sonication at 30% amplitude for 10 s with 0.5 s on and off pulses using a 3-mm microtip (Sonics Vibra-Cell, Newtown, CT). The primary emulsion was poured into 100 ml of a cold 1% aqueous polyvinyl alcohol solution and homogenized (L4RT, Silverson Machines, East Longmeadow, MA) for 2 min to form a double emulsion. The polymeric microparticles were continuously stirred for 2.5 h to allow hardening due to solvent evaporation, collected by centrifugation, washed three times with reverse-osmosis water and freeze-dried into a freely flowing powder. For confocal images, 50 mg/ml FITC-dextran (20 kDa) was encapsulated by adding it to the inner aqueous phase during particle formation. For surface analysis, particles were washed 10 times with double-distilled water before freeze-drying.

2.6. Imaging of microparticles by DIC, fluorescence and scanning electron microscopy

Differential interference contrast (DIC) and fluorescence images of drug carriers were acquired with a laser scanning confocal microscope (Zeiss LSM 510 Meta, New York, NY) equipped with a 100 \times oil immersion lens and a 488-nm laser line. Samples were prepared by suspending 5–10 mg of particles in 1 ml

water, then placing the particle suspension between a glass slide and coverslip.

Aerosol particle surface morphology was evaluated by scanning electron microscopy (SEM) with a Jeol JSM-6700F cold cathode field emission SEM (Peabody, MA). Microparticle samples were attached to SEM mounts using double-sided graphite carbon tape and sputter coated with platinum at 0.5 nm/min for 5 min using a Polaron Range SC7640 Sputter Coater (Quorum Technologies, Newhaven, England). Populations representative of each microsphere sample were photographed.

2.7. Microparticle bulk characterization (size, density and water content)

The volume–mean size distribution and geometric standard deviation (GSD) of microparticles were determined using a Coulter Multisizer IIe (Beckman-Coulter Fullerton, CA). To allow calculation of the theoretical particle mass–mean aerodynamic diameter (see Eq. (2) in Section 3), all particles within a given formulation were assumed to possess roughly the same density. Therefore, the volume–mean particle diameter was approximated as roughly equal to the mass–mean diameter. Approximately 2 ml of isoton II solution was added to 5–10 mg microparticles. The solution was briefly vortexed to suspend the microparticles and added dropwise to 100 ml of isoton II solution until the coincidence of particles was between 8% and 10%. Greater than 100,000 particles were sized for each batch of microparticles to determine the mean particle size and size distribution. The bulk density of the particles was determined by tap density measurements. Briefly, particles were loaded into 0.3-ml sections of a 1-ml plastic pipette, capped with NMR tube caps and tapped approximately 300–500 times on a hard benchtop until the volume of the powder did not change. The tap density was determined from the difference between the weight of the pipette before and after loading, divided by the volume of powder after tapping.

Thermogravimetric analysis was conducted to determine particle water content using a TA Instruments SDT 2960 apparatus (10 $^{\circ}$ C/min, 25–250 $^{\circ}$ C; New Castle, DE) on 6–12-mg samples under nitrogen purge.

2.8. Microparticle surface analysis (surface charge and chemical composition)

Particle surface charge was determined by zeta potential measurements (Malvern Zetasizer 3000, Southborough, MA). Samples were prepared by diluting approximately 0.5–1 mg of particles in 3 ml of 1 mM NaCl.

X-ray photoelectron spectroscopy (XPS) was performed using a Kratos Analytical Axis Ultra XPS (Chestnut Ridge, NY) with a monochromatic aluminum X-ray source. Samples were stored at -5°C under desiccant until 1 h prior to analysis, at which point they were allowed to come to room temperature. Samples were mounted on double sided adhesive carbon tape and analyzed in duplicate. The approximate sampling depth was 25 Å.

2.9. In vitro aerosolization of microparticles

Microparticle aerodynamic characteristics were studied in vitro using an Andersen Mark II Cascade Impactor (Graseby Andersen, Smyrna, GA) at an air flow rate of 28.3 l/min. Cut-off particle aerodynamic diameters for each stage of the impactor at this flow rate were: stage 0 (10.00 μm), stage 1 (9.00 μm), stage 2 (5.80 μm), stage 3 (4.70 μm), stage 4 (3.30 μm), stage 5 (2.10 μm), stage 6 (1.10 μm), stage 7 (0.65 μm) and filter (0.43 μm). Particles were aerosolized from #2 gelatin capsules (Eli Lilly, Indianapolis, IN) using a Spinhaler dry powder inhaler (DPI; Fisons, Bedford, MA). To minimize particle bouncing [14], the metal impaction plates were dipped in an acetone solution containing 2 wt.% Tween 80 and dried at 80°C for at least 2 h to create a thin surface film. In studies using lactose as a carrier, 10% microparticles by weight were vortexed as a dry powder with a fine particle fraction of lactose for 30 min prior to aerosolization. SEM was performed on several lactose/particle formulations to confirm blend uniformity. All polymer particle types mixed well with lactose particles. The lactose powder had a volume mean diameter of $33.5 \pm 0.3 \mu\text{m}$ after sieving through a 75- μm sieve, as determined using a Mastersizer S (Malvern Instruments, Southborough, MA).

Microparticles deposited on each of nine stages of the impactor were collected in petri dishes by carefully washing the plates with 0.8 N NaOH solution.

The NaOH solution provided rapid degradation of the polymer and dissolution of the encapsulated fluorescent material (rhodamine B base). The impactor neck was rinsed with 100% ethanol. The neck sample was vacuum dried overnight, then dissolved in 0.8 N NaOH. After 3 h of incubation at 37°C , the amount of fluorescent material on each stage was measured at 550 nm (excitation) and 570–700 nm (emission) using a fluorometer (Turner Designs, Sunnyvale, CA). Emitted dose (ED), the percentage of particles that exited the inhaler and FPF, and the percentage of aerosolized particles that reached the lower five stages of the impactor (corresponding to aerodynamic diameters below 4.7 μm) were then calculated. Significant ($p < 0.05$) differences in ED and FPF values from $n = 3$ data points were determined by one-way analysis of variances (ANOVA).

3. Results

3.1. Characterization of poly(ether-anhydrides)

A family of polymers with various percentages of PEG randomly copolymerized with SA were synthesized by hot melt polycondensation. Polymers were characterized by GPC to determine their weight (M_w)– and number (M_n)–average molecular weights and polydispersity index (PDI) (Table 1). All GPC chromatographs contained one peak corresponding to the polymer. No smaller M_w fragments, such as unreacted PEG (8000 Da), were evident. The average polymer M_w varied slightly with the percentage of PEG in the polymer backbone. In this study, copolymers containing roughly 10 wt.% PEG and 90 wt.% SA [poly(PEG:SA//10:90)] had a M_w of 26.6 kDa, whereas poly(SA) had a M_w of 22.9 kDa and poly(-PEG:SA//30:70) had a M_w of 18.7 kDa. The PDI ranged between 1.8 and 1.9 for all polymers, indicat-

Table 1
Polymer characterization

Polymer	MW ^a (Da)	PDI ^a	Contact angle
Poly(SA)	22,900	1.86	$81.4 \pm 5.2^{\circ}$
Poly(PEG:SA//10:90)	26,600	1.83	$56.7 \pm 4.9^{\circ}$
Poly(PEG:SA//30:70)	18,700	1.92	$46.1 \pm 0.9^{\circ}$

^a Determined by GPC analysis.

ing that the polymer chains possessed a low degree of polydispersity.

The relative hydrophilicity of the polymers as a function of PEG content was determined by contact angle measurements (Table 1). The hydrophilicity of the polymer increased with increasing amounts of PEG in the polymer backbone, as evidenced by a decrease in the water contact angle from 81° for poly(SA), to 57° for poly(PEG:SA//10:90), to 46° for poly(PEG:SA//30:70). Polymeric particles containing PEG are expected to be more hydrophilic than the polymer films tested since PEG partitions into the external aqueous phase (i.e., to the particle surface) during particle preparation [15–17]. The presence of a dense PEG coating on the surfaces of poly(ether-anhydride) microparticles was recently confirmed by confocal microscopy with fluorescently labeled PEG [15].

3.2. Particle size and GSD

The mass–mean geometric size and GSD of each batch of polymeric particles were determined by sizing greater than 100,000 particles (Table 2). The GSD was determined from the following equation [18]:

$$\text{GSD} = \frac{d_{84\%}}{d_{50\%}} \quad (1)$$

where d_n is the diameter at the n th percentile of the cumulative distribution. The mass–mean size of polymeric microparticles used to determine the effect of %PEG in the polymer on resulting particle aerodynamic behavior, ranged between 7.5 and 8.1 μm , with

a GSD of 1.4–1.5. Typical GSD values for aerosol particles are 1.3–3.0 [19–21]. The mass–mean aerodynamic diameters (d_{aero}) of the polymeric particles, determined from the particle mass–mean size and tap density, ranged between 4.0 and 4.6 μm (Table 2) as found from the relationship:

$$d_{\text{aero}} = \frac{d}{\gamma} \sqrt{\rho/\rho_a} \quad (2)$$

where d = geometric diameter, γ = shape factor = 1 for a sphere, ρ = particle bulk density (g/ml) and ρ_a = water mass density (1 g/ml). Particles with d_{aero} between 2 and 5 μm that are inhaled via the mouth are capable of efficient alveolar deposition [22,23], whereas d_{aero} between 4 and 10 μm result in deposition primarily in the tracheobronchial regions of the lungs. Therefore, particles with d_{aero} in the 4.0–4.6 μm range are expected to deposit in both the alveolar and tracheobronchial regions of the lungs [12], assuming they can be aerosolized as single particles as opposed to aggregates. It is noted that tap density measurements underestimate particle bulk densities since the volume of particles measured includes the interstitial space between the particles. Therefore, true particle densities, and thus aerodynamic diameters, are expected to be slightly larger than reported (shifting expected particle deposition slightly toward the upper impactor stages that correspond to the upper lungs).

3.3. Effect of polymer PEG content on particle aerosolization

Particles made using polymers with varying %PEG were loaded (\pm lactose carrier particles) into gelatin capsules and aerosolized into an Andersen Cascade Impactor at a flow rate of 28.3 l/min in all studies. ED of 80–92% were obtained for all particles in the aerodynamic size range of 4.0–4.5 μm , regardless of surface chemistry (Fig. 1A). Only the emitted doses of poly(SA) (80% ED without lactose) and poly(PEG:SA//30:70) (89% ED without lactose) were statistically different ($p < 0.01$). FPF of these particles (Fig. 1B) increased from 9.1% [poly(SA)] to 16.1% [poly(PEG:SA//10:90)] with the addition of 10% PEG into the polymer backbone ($p < 0.03$), and then decreased to 12.8% [poly(PEG:SA//30:70)] with 30% PEG polymer particles ($p < 0.03$ compared to

Table 2
Characterization of microparticle physical properties (varying %PEG)

Particle type	Size \pm S.E.M. (μm)	Density (g/cm^3)	$d_{\text{aero}}^{\text{a}}$ (μm)	GSD ^b (μm)
Poly(SA)	7.5 \pm 1.6	0.357	4.5	1.5
Poly(PEG:SA// 10:90)	8.1 \pm 1.5	0.251	4.0	1.4
Poly(PEG:SA// 30:70)	8.1 \pm 1.7	0.317	4.6	1.5

^a Calculated using Eq. (2) from the average size and bulk density of the particles.

^b Calculated using Eq. (1) from the size distribution of the particles.

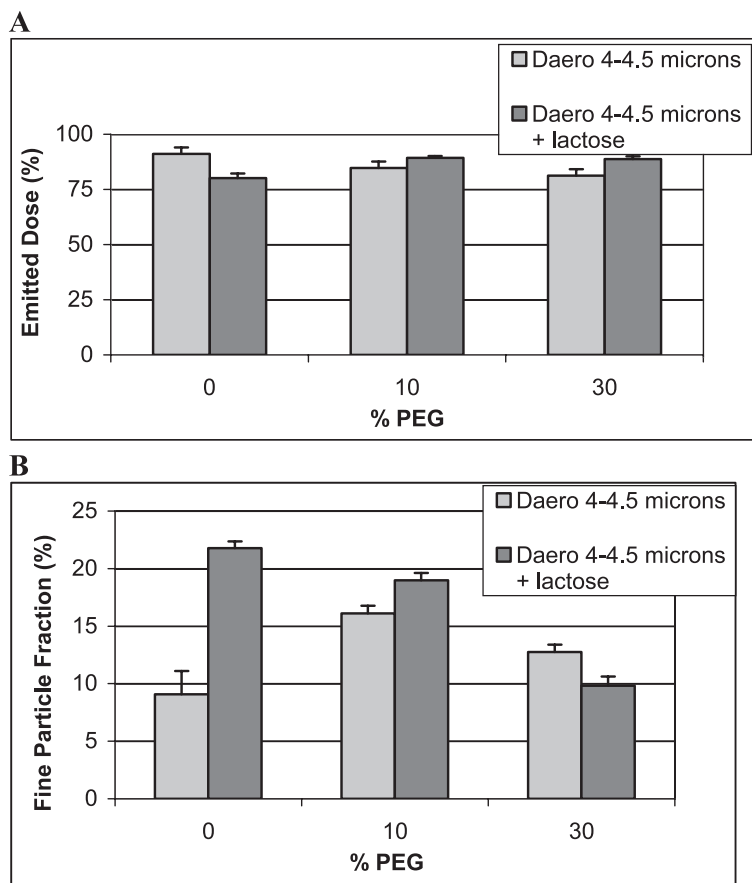


Fig. 1. Effect of %PEG and lactose on (A) particle aerosolization and (B) deposition in an in vitro lung model.

PEG:SA//10:90 particles). Poly(SA) and poly(-PEG:SA//30:70) FPFs were not statistically different. The addition of lactose particles ($33.5 \pm 0.3 \mu\text{m}$) mixed with poly(SA) microparticles more than doubled their FPF to 21.8% ($p < 0.01$). Lactose increased the FPF of poly(PEG:SA//10:90) microparticles only slightly, from 16.5% to 19.0% ($p < 0.04$), and decreased the FPF of poly(PEG:SA//30:70) microparticles from 12.8% to 9.8% ($p < 0.03$).

3.4. Effect of aerodynamic size on particle aerosolization

To determine the effect of poly(ether-anhydride) particle aerodynamic size on aerosolization and deposition, poly(PEG:SA//10:90) particles with aerodynamic diameters of 2.7, 3.4 and 4.0 μm were

produced (Table 3). Microparticle size had no significant effect on the ED of poly(PEG:SA//10:90) particles in the aerodynamic size range of 2.7–4.0 μm (Fig. 2A). In addition, a change in aerodynamic

Table 3
Characterization of poly(PEG:SA//10:90) microparticle physical properties (varying aerodynamic size)

Size \pm S.E.M. (μm)	Density (g/cm^3)	$d_{\text{aero}}^{\text{a}}$ (μm)	GSD ^b (μm)
4.4 ± 0.1	0.380	2.7	1.6
6.3 ± 1.7	0.290	3.4	1.6
8.1 ± 1.5	0.317	4.0	1.4

^a Calculated using Eq. (2) from the average size and bulk density of the particles.

^b Calculated using Eq. (1) from the size distribution of the particles.

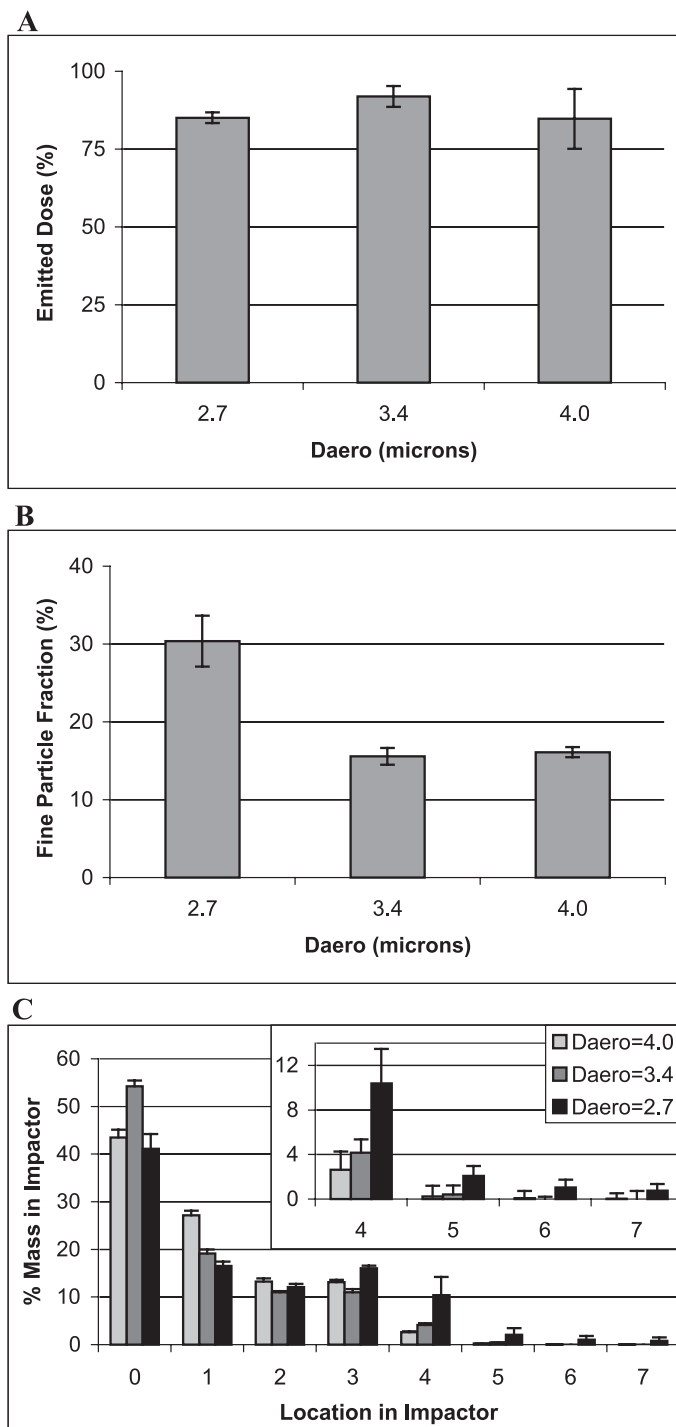


Fig. 2. Effect of poly(PEG:SA//10:90) particle aerodynamic size on (A) emitted dose, (B) fine particle fraction and (C) deposition patterns in an in vitro lung model.

diameter from 4.0 to 3.4 μm caused no statistically significant change in the fine particle fraction in the in vitro lung model (Fig. 2B). However, a decrease in aerodynamic diameter to 2.7 μm nearly doubled the FPF, from 16% to 30% ($p < 0.02$ compared to either 3.4 or 4.0 μm particles) (Fig. 2B), as demonstrated by a shift in the deposition pattern towards the lower stages of the impactor (stages 3–7) (Fig. 2C).

3.5. Particle shape and surface roughness

Confocal and light microscopy images (Fig. 3) show a significant difference in internal structure between the poly(SA) microparticles and poly(PEG:SA) microparticles. Poly(SA) particles have smooth surfaces and a thin outer polymer shell, with the model drug FITC-dextran evenly distributed within the inner core of the particles. On the other hand, poly(PEG:SA//10:90) microparticles have a globular internal structure, with the drug distributed in small pockets throughout the particle (presumably corresponding to the water phase of the primary emulsion). Poly(PEG:SA//30:70) microparticles exhibited a mix of the two types of internal structures.

SEM showed that all formulations produced mainly spherical particles (Fig. 4). Poly(SA) microparticles had slightly textured, but relatively smooth surfaces (Fig. 4A). Polymers containing 10% PEG produced particles with rougher surfaces and holes that penetrated into the particle (Fig. 4B). Particles made with polymers containing 30% PEG appeared smoother

than the 10% PEG polymer particles, but had noticeably larger holes (Fig. 4C). SEM on a mixture of lactose particles and polymer microparticles showed very large, blocky lactose particles with many smaller microparticles attached, typically at the edges and crevices (Fig. 4D). Particles were rarely attached to the flat planes of the lactose particles unless smaller lactose particles were present on those surfaces.

3.6. Particle surface charge and chemical composition

Poly(SA) and poly(PEG:SA//10:90) particles used in aerosolization studies exhibited surface charges of approximately -13 mV (Table 4), as measured using a Zetasizer. Poly(PEG:SA//30:70) particles exhibited a more negative surface charge of -20 mV. In order to explain zeta potential data, microparticle surface composition was analyzed by XPS. An equal percentage (22%) of the detected signal for poly(SA) and poly(PEG:SA//10:90) microparticles was attributed to DPPC, a surfactant used during particle formation (Table 4). However, no DPPC was observed on the surfaces of poly(PEG:SA//30:70) particles, where DPPC may be excluded from the surface due to competition with PEG. Zeta potential data for microparticles made without DPPC confirmed that the surface charge is more neutral for 10% PEG polymer particles [-40 mV for poly(SA) compared to -20 mV for poly(PEG:SA//10:90)] (Table 4). No additional change in zeta potential was observed when polymers composed of 30% PEG were used to produce

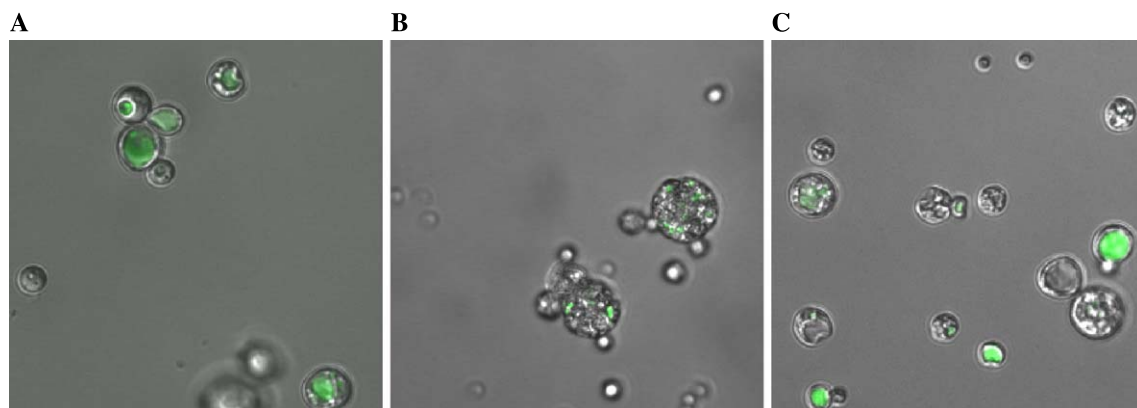


Fig. 3. Confocal images overlaid with light microscopy images showing the internal texture of polymeric microparticles and the location of FITC-dextran encapsulated within the particles: (A) poly(SA), (B) poly(PEG:SA//10:90), (C) poly(PEG:SA//30:70) microparticles.

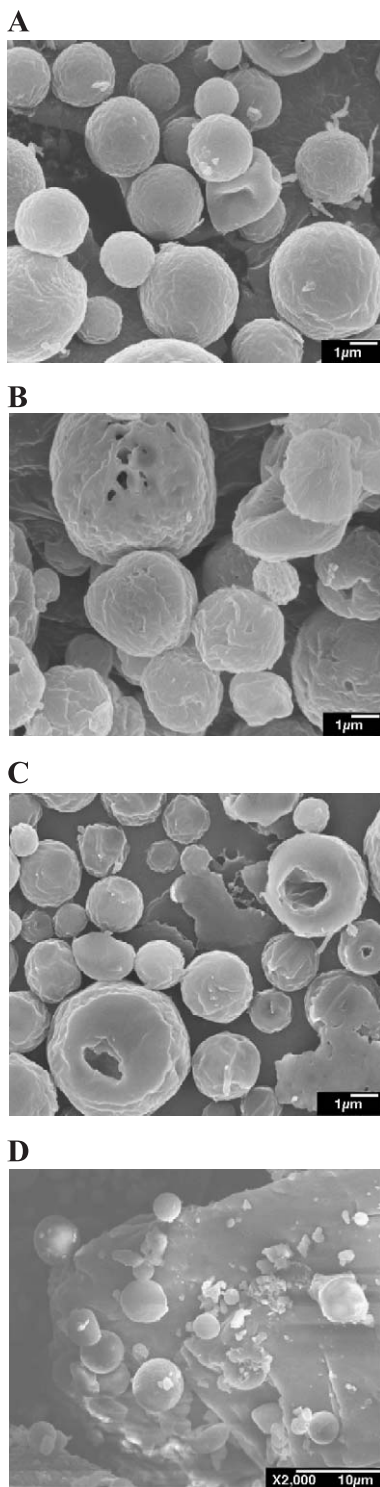


Table 4

Characterization of microparticle chemical properties (varying %PEG)

Particle type	Particles containing DPPC			No DPPC
	Surface charge ^a	%DPPC ^b on surface	Water content (%) ^c	Surface charge ^a
Poly(SA)	-13.3 ± 3.0	22	0.22	-40.2 ± 6.4
Poly(PEG:SA//10:90)	-12.6 ± 1.9	22	0.10	-20.2 ± 0.3
Poly(PEG:SA//30:70)	-20.2 ± 0.8	0	0.23	-21.4 ± 0.8

^a Determined by zeta potential measurements.

^b Determined by XPS analysis.

^c Determined by TGA analysis.

particles; poly(PEG:SA//30:70) microparticles with and without DPPC exhibited identical zeta potentials of -20 mV. Thus, DPPC appears to partially mask the surface charge of polymeric particles containing 10% PEG or less.

3.7. Water content of particles

The water content of microparticles, as determined by TGA analysis, varied with particle composition (Table 4). Poly(SA) and poly(PEG:SA//30:70) particles used in aerosolization studies had similar water contents of 0.22 and 0.23 wt.%, respectively, whereas poly(PEG:SA//10:90) particles exhibited a lower water content of 0.10 wt.%. The TGA apparatus used has a resolution of 0.1 μ g; therefore, a difference of 0.01% for approximately 5–10 mg samples is considered statistically significant.

4. Discussion

A new family of ether-anhydride terpolymers composed of PEG, SA and CPP has been recently developed for drug delivery following injection or inhalation [8,9]. These polymers were designed to overcome many of the limitations of currently available off-the-shelf polymers, such as poly(lactide-co-

Fig. 4. Scanning electron microscopy images showing the external surface structure of (A) poly(SA), (B) poly(PEG:SA//10:90) and (C) poly(PEG:SA//30:70) microparticles (bar = 1 μ m, $\times 6000$), and (D) poly(SA) microparticles attached to lactose (bar = 10 μ m, $\times 2000$).

glycolide) (PLGA). The PEG-containing poly(ether-anhydrides) synthesized here have significantly shorter degradation times, ranging from hours to many days depending on composition, and thus may be more appropriate for intravenous or pulmonary drug delivery than PLGA [8,9]. Although degradation of the anhydride bonds occurs fairly rapidly, the removal rate of the oligomers and monomers is mainly dissolution-controlled [24]. Thus, poly(ether-anhydrides) can be manipulated to erode at predictable rates (from several hours to weeks) and steadily release therapeutic drugs throughout the erosion period [9]. PEG is a biocompatible material that allowed control of the surface properties of polymer particles, which in turn increased polymer degradation rates and decreased particle removal rates by phagocytosis (unpublished results). In this paper, particle aerosolization efficiency is shown to be significantly improved by simply varying the PEG content of PEG:SA polymers used to produce the aerosol particles.

Aerosol particles aggregate when a net adhesive energy exists between the particles (primarily due to VDW, electrostatic and capillary forces between dry powder aerosol particles [18,25]) and remain aggregated if the shear forces created during inhalation do not exceed the forces holding the particles together. In these studies, large, low density particles were prepared with ether-anhydride polymers since they exhibit superior aerosolization efficiencies compared to traditional small dense particles [6,7], presumably due to decreased net van der Waals (VDW) forces. A decrease in net VDW forces as particle diameter increases can be readily seen when the VDW force is considered on a per mass of particles basis (in which case $F_{vdw} \sim 1/d^2$, where d = geometric diameter). Large, low density particles were prepared from polymers containing varying percentages of PEG built into the backbone structure in order to decrease interparticle adhesion further. PEG is a relatively hydrophilic monomer (compared to CPP and SA) that is known to partition to oil–water interfaces during the emulsion process used to produce particles and, therefore, to segregate to particle surfaces [15–17].

Emitted doses of 80–92% were obtained for poly(PEG:SA) particles in the aerodynamic size range of 4.0–4.6 μm (Fig. 1A), indicating they are able to deaggregate sufficiently to leave the capsule and

inhaler. However, particles made with polymers containing 10% PEG exhibited significantly higher FPF than those made with 0% or 30% PEG (Fig. 1B). To gain insight into the effect of poly(ether-anhydride) particle physico-chemical properties on aerosolization efficiency, the following was determined for each particle batch: particle shape and surface roughness (potentially related to VDW, capillary and electrostatic forces), surface charge (electrostatic forces), surface chemical composition (VDW and capillary) and bulk water content (capillary). Each of these factors can have a significant effect on the strength of particle–particle interactions that lead to aggregation and inefficient aerosolization.

All particles were spherical in shape, however, those prepared with polymers containing either 0% or 30% PEG possessed noticeably smoother surfaces compared to 10% PEG particles (Fig. 4). Smoother surfaces may have increased particle–particle contact for 0% and 30% PEG particles, thereby increasing their aggregation by potentially any of the forces that promote interparticle adhesion (VDW, capillary or electrostatic) [26,27]. This result is consistent with the reduced FPFs observed for 0% and 30% PEG particles compared to 10% PEG particles.

Contact angle measurements and XPS were performed to gain insight into the potential effects of surface chemical composition on particle–particle interactions that may limit efficient aerosolization. The contact angle decreased as the percentage of PEG in the polymer increased, demonstrating that PEG incorporation increased the hydrophilicity. High surface energy materials (in air, this generally corresponds to more hydrophilic materials) [28] exhibit higher VDW attractive forces. This result, if considered alone, would suggest that higher FPFs would be achieved for the poly(SA) particles. Since particles composed of 10% PEG polymers exhibited significantly higher FPFs, it is possible that VDW adhesive forces owing to particle surface energy do not dominate their adhesion. This result is not conclusive, however, since it is also possible that the poly(SA) particles may have been coated with a higher amount of PVA, a highly hydrophilic and hygroscopic surfactant used during particle preparation, relative to the PEG-containing particles. PVA is known to adsorb strongly to the surfaces of hydrophobic PLGA particles [29], but may not adsorb as strongly to PEG-

containing particles. In this case, the poly(SA) particles would possess the highest surface energy in air of those tested, which should translate into lower FPFs. Unfortunately, the percentages of PVA, poly(SA) and PEG on the surfaces of the particles could not be distinguished with sufficient confidence. Future studies with high-resolution XPS, similar to those performed by Shakesheff et al. [29], are planned.

Water on particle surfaces masks surface charge and can create strong adhesive capillary forces due to the formation of water bridges between particle surfaces [30]. Water content was higher for 0% and 30% PEG particles compared to 10% PEG particles (Table 4), suggesting that aggregation due to capillary forces may be reduced for 10% PEG particles. Generally, more hydrophilic or hygroscopic materials favor the adsorption of water. Particles composed of pure poly(SA) are very hydrophobic, suggesting they should have a relatively low water content. Therefore, the higher water content of the poly(SA) particles compared to 10% PEG particles suggests that relatively more PVA, a hydrophilic surfactant, is likely adsorbed to the poly(SA) particle surface. Water adsorption is expected to reduce particle aerosolization efficiency primarily by causing particle aggregation during storage owing to the high particle packing densities in capsules and blister packs. Water adsorption following aerosolization into the humid lungs [31,32] may also increase particle aggregation for more hygroscopic materials, thereby further reducing particle flight into the deeper regions.

Electrostatic forces can be larger than VDW forces if the particles are charged [33]. These forces are adhesive between oppositely charged particles and repulsive between similarly charged particles. It is interesting to note that the poly(PEG:SA//30:70) microparticles used in aerosolization studies possessed a more highly negative surface charge than either poly(SA) or poly(PEG:SA//10:90) particles (Table 4), suggesting that 30% PEG particles may benefit from increased electrostatic repulsion. However, since the 30% PEG particles did not deposit more efficiently into the deeper stages of the model lung compared to the 10% PEG particles (Fig. 1B), it appears that electrostatics did not play a major role in the adhesion of poly(ether-anhydride) particles.

Finally, it is important to note that PEG on particle surfaces can also induce a repulsive steric interaction

between particles that could effectively decrease the overall adhesive forces [34–36], thereby allowing more efficient aerosolization and stabilizing the colloidal suspension in air. The steric repulsion created with the addition of 10% PEG to the polymer backbone of the particles may allow more efficient deaggregation of the particles, thereby increasing deposition. However, if steric repulsion plays a significant role, then other adhesive forces between 30% PEG particles dominate since 30% PEG particles exhibited lower FPFs compared to 10% PEG particles.

In another experiment, a decrease in poly(PEG:SA//10:90) microparticle aerodynamic diameter from 4.0 to 3.4 μm caused no change in FPF (Fig. 2B). This result is not surprising considering the cut-off diameters of the cascade impactor stages targeted by these particle sizes. Particles of aerodynamic diameters of 3.3–4.7 μm should deposit primarily on the third stage of the impactor. Poly(ether-anhydride) microparticles with average aerodynamic diameters of 4.0 and 3.4 μm mainly deposited on stages 3 and above (Fig. 2C). However, a decrease in aerodynamic diameter to 2.7 μm doubled the FPF from 16% to 30% and shifted the deposition pattern towards the fourth stage of the impactor (Fig. 2C), as theoretically expected. Complete deaggregation of the particles was not achieved, however, as indicated by significant particle deposition on the upper stages of the impactor (Fig. 2C). It should be noted, however, that FPFs in the range of 30% are significant considering the suboptimal, currently obsolete dry powder inhaler used in this study. Also, extensive studies were not performed to optimize FPFs further. Rather, the goal of this study was to determine if ED and FPF could be significantly affected for the new polymer aerosol drug carriers by simply varying the percentage of the monomers used to produce the polymers.

Large carrier particles, typically composed of sugars such as lactose, are commonly used to increase the fraction of drug or particles that reaches the deep lung following inhalation. By SEM, it appeared that the polymer microparticles preferentially adhered to lactose particles at the edges and crevices on the lactose surface, where the surface was very rough (Fig. 4D). Particles were rarely seen on the flat planes of the lactose, suggesting that poly(ether-anhydride) particles needed multiple attachment points to remain

adhered to the lactose particles. The addition of a fine particle fraction of lactose to poly(SA) particles increased the FPF by up to an additional 100% (Fig. 1B). However, lactose added to particles containing 10% PEG produced only a small improvement in FPF, from 16.5% (no lactose) to 19.0% (with lactose). The addition of lactose to particles containing 30% PEG in the polymer backbone led to a decrease in the FPF from 12.8% (no lactose) to 9.8% (with lactose), suggesting that PEG-containing particles may inefficiently detach from the lactose carrier.

5. Conclusions

Biodegradable poly(ether-anhydride) microparticles have been designed for drug delivery following aerosolization into the lungs. PEG added to the polymer backbone significantly changed particle hydrophilicity, surface roughness, surface charge and water content and may provide a steric barrier to reduce particle aggregation. The addition of 10% PEG into the polymer backbone appears to reduce important interparticle adhesion forces, as supported by their significantly increased deposition in deeper stages of a model lung following aerosolization as a dry powder compared to 0% or 30% PEG particles. The decreased FPF obtained with 30% PEG particles compared to 10% PEG particles is likely due to decreased surface roughness or increased capillary forces. The use of lactose as a carrier for the microparticles provided an additional increase in the fine particle fractions for particles containing 0% and 10% PEG. High fine particle fractions with an obsolete inhaler, the use of monomers currently used in products approved for human use (albeit not yet in the lungs), and the ability to release various drug molecules in a sustained fashion [9], make poly(ether-anhydride) particles promising for inhalation therapy.

Acknowledgements

The authors thank Junghae Suh for help in obtaining confocal and light microscopy images, and Katrin Johannsen, Daniel Callahan and Claire Jeong for technical assistance. XPS and TGA analysis was performed at the Materials Characterization Labora-

tory at the Pennsylvania State University. This work was partially supported by The Whitaker Foundation (RG 990046) and by a fellowship to J. Fiegel from the National Science Foundation (DGE 9616062).

References

- [1] R.U. Agu, M.I. Ugwoke, M. Armand, R. Kinget, N. Verbeke, The lung as a route for systemic delivery of therapeutic proteins and peptides, *Respir. Res.* 2 (2001) 198–209.
- [2] B. Damms, W. Bains, The cost of delivering drugs without needles, *Bio-Technol.* 13 (1995) 1438–1440.
- [3] J.S. Patton, J. Bukar, S. Nagarajan, Inhaled insulin, *Adv. Drug Deliv. Rev.* 35 (1999) 235–247.
- [4] J.S. Patton, Pulmonary delivery of drugs for bone disorders, *Adv. Drug Deliv. Rev.* 42 (2000) 239–248.
- [5] J.L. Selam, Inhaled insulin: clinical results in type 2 diabetic patients, *Diabetes Metab.* 27 (2001) S28–SA32.
- [6] D.A. Edwards, J. Hanes, G. Caponetti, J. Hrkach, A. Ben-Jebria, M.L. Eskew, J. Mintzes, D. Deaver, N. Lotan, R. Langer, Large porous particles for pulmonary drug delivery, *Science* 276 (1997) 1868–1871.
- [7] J. Hanes, D.A. Edwards, C. Evora, R. Langer, Particles incorporating surfactants for pulmonary drug delivery, U.S. Patent No. 5,855,913, 1999.
- [8] J. Fu, J. Fiegel, E. Krauland, J. Hanes, New polymeric carriers for controlled drug delivery following inhalation or injection, *Biomaterials* 23 (2002) 4425–4433.
- [9] J. Fu, J. Fiegel, J. Hanes, Synthesis and characterization of PEG-based ether-anhydride terpolymers: novel polymers for controlled drug delivery, submitted.
- [10] R.P. Batycky, J. Hanes, R. Langer, D.A. Edwards, A theoretical model of erosion and macromolecular drug release from biodegrading microspheres, *J. Pharm. Sci.* 86 (1997) 1464–1477.
- [11] B.S. Neumann, in: H.S. Bean, A.H. Beckett, J.E. Carless (Eds.), *Advances in Pharmaceutical Sciences*, Academic Press, London, 1967, pp. 181–221.
- [12] H. Landahl, On the removal of air-borne droplets by the human respiratory tract: I. The lung, *Bull. Math. Biophys.* 12 (1950) 43–56.
- [13] J. Fiegel, C. Ehrhardt, U.F. Schaefer, C.-M. Lehr, J. Hanes, Large porous particle impingement on lung epithelial cell monolayers—toward improved particle characterization in the lung, *Pharm. Res.* 20 (2003) 788–796.
- [14] J. Turner, S. Hering, Greased and oiled substrates as bounce-free impaction surfaces, *J. Aerosol Sci.* 18 (1987) 215–224.
- [15] J. Fu, H.S. Sakhalkar, D.J. Goetz, J. Hanes, in preparation.
- [16] R. Gref, Y. Minamitake, M.T. Peracchia, V. Trubetskoy, V. Torchilin, R. Langer, Biodegradable long-circulating polymeric nanospheres, *Science* 263 (1994) 1600–1603.
- [17] M.T. Peracchia, R. Gref, Y. Minamitake, A. Domb, N. Lotan, R. Langer, PEG-coated nanospheres from amphiphilic diblock and multiblock copolymers: investigation of their drug encapsulation and release characteristics, *J. Control. Release* 46 (1997) 223–231.

- [18] W.C. Hinds, *Aerosol Technology: Properties, Behavior, and Measurement of Airborne Particles*, 2nd ed., Wiley, New York, NY, 1999.
- [19] J. Ferin, G. Oberdoerster, D.P. Penney, Pulmonary retention of ultrafine and fine particles in rats, *Am. J. Respir. Cell Mol. Biol.* 6 (1992) 535–542.
- [20] P. O'Hara, A.J. Hickey, Respirable PLGA microspheres containing rifampicin for the treatment of tuberculosis, *Pharm. Res.* 17 (2000) 955–961.
- [21] R. Vanbever, A. Ben-Jebria, J.D. Mintzes, R. Langer, D.A. Edwards, Sustained release of insulin from insoluble inhaled particles, *Drug Dev. Res.* 48 (1999) 178–185.
- [22] H. Schulz, Mechanisms and factors affecting intrapulmonary particle deposition: implications for efficient inhalation therapies, *Pharm. Sci. Technol. Today* 1 (1998) 336–344.
- [23] M. Lippmann, R.E. Albert, The effect of particle size on the regional deposition of inhaled aerosols in the human respiratory tract, *Am. Ind. Hyg. Assoc. J.* 30 (1969) 257–275.
- [24] A. Göpferich, J. Tessmar, Polyanhydride degradation and erosion, *Adv. Drug Deliv. Rev.* 54 (2002) 911–931.
- [25] K. Gotoh, H. Masuda, K. Higashitani, *Powder Technology Handbook*, 2nd ed., Marcel Dekker, New York, NY, 1997.
- [26] D. Maugis, On the contact and adhesion of rough surfaces, *J. Adhes. Sci. Technol.* 10 (1996) 161–175.
- [27] D. Tabor, Surface forces and surface interactions, *J. Colloid Interface Sci.* 58 (1977) 2–13.
- [28] J. Visser, Van der Waals and other cohesive forces affecting powder fluidization, *Powder Technol.* 58 (1989) 1–10.
- [29] K.M. Shakesheff, C. Evora, I. Soriano, R. Langer, The adsorption of poly(vinyl alcohol) to biodegradable microparticles studied by X-ray photoelectron microscopy (XPS), *J. Colloid Interface Sci.* 185 (1997) 538–547.
- [30] A.J. Hickey, N.M. Concessio, M.M. Van Oort, R.M. Platz, Factors influencing the dispersion of dry powders as aerosols, *Pharm. Technol.* (1994) 58.
- [31] W.H. Finlay, *The Mechanisms of Inhaled Pharmaceutical Aerosols*, Academic Press, San Diego, CA, 2001.
- [32] F. Podczeczek, J.M. Newton, M.B. James, Variations in the adhesion force between a drug and carrier particles as a result of changes in the relative humidity of the air, *Int. J. Pharm.* 149 (1997) 151–160.
- [33] W.H. Marlow, in: W.H. Marlow (Ed.), *Aerosol Microphysics: I. Particle Interaction*, McGraw-Hill, New York, NY, 1980, pp. 116–156.
- [34] P. Somasundaran, X. Yu, S. Krishnakumar, Role of conformation and orientation of surfactants and polymers in controlling flocculation and dispersion of aqueous and non-aqueous suspensions, *Colloids Surf.* 133 (1998) 125–133.
- [35] A.G.A. Coombes, S. Tasker, M. Lindblad, J. Holmgren, K. Hoste, V. Toncheva, E. Schacht, M.C. Davies, L. Illum, S.S. Davis, Biodegradable polymeric microparticles for drug delivery and vaccine formulation: the surface attachment of hydrophilic species using the concept of poly(ethylene glycol) anchoring segments, *Biomaterials* 18 (1997) 1153–1161.
- [36] W. Lin, M.C. Garnett, M.C. Davies, F. Bignotti, P. Ferruti, S.S. Davis, L. Illum, Preparation of surface-modified albumin nanospheres, *Biomaterials* 18 (1997) 559–565.